Bioconjugate Chemistry

Article

pubs.acs.org/bc

Affinity-Guided Covalent Conjugation Reactions Based on PDZ–Peptide and SH3–Peptide Interactions

Yao Lu, Feng Huang, Jianpeng Wang, and Jiang Xia*

Department of Chemistry, The Chinese University of Hong Kong, Shatin, Hong Kong SAR, China

Supporting Information

ABSTRACT: Specific protein–peptide interactions are prevalent in the living cells and form a tightly regulated signaling network. These interactions, many of which have structural information revealed, provide ideal templates for affinity-guided covalent bioconjugation. Here we report the development of a set of four new reactions that covalently and site-specifically link nonenzymatic scaffolding domains (two PDZ and two SH3 domains) and their ligands through thiol-chloroacetyl S_N2 reaction. Guided by the three-dimensional structure of the wild type complex, a selected position of the protein was mutated to cysteine, and at the same time, an α-chloroacetyl group was installed at a corresponding position of the peptide. Specific binding interaction between the two brings the reactive groups into close proximity, converts the nonreactive cysteine residue into a content-dependent reactive site, and induces the nucleophilic reaction that is inert in the absence of the binding event. The specificity, orthogonality, and modularity of the four reactions were characterized, the reaction was applied to label proteins *in vitro* and receptor on the surface of mammalian cells, and the system was utilized to assemble covalent protein complexes with unnatural geometries.

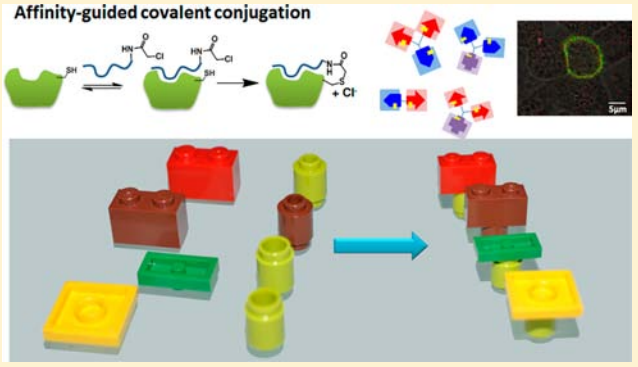

INTRODUCTION

A multitude of bioconjugation reactions have been developed to install nonproteinaceous chemical groups at particular sites of proteins, thereby expanding the scope of protein chemistry beyond the 20 natural amino acids.[1] Affinity-guided covalent conjugation, a.k.a. ligand-directed reaction, represents a particularly interesting type of bioconjugation reaction due to their distinct features including spontaneity, rapid reaction rate, biocompatibility, site-specificity, and versatility. This strategy starts from reversible and noncovalent binding interaction of the protein and the synthetic ligand; the binding interaction accurately positions a reactive functional group preinstalled in the ligand (e.g., an electrophile) to the vicinity of a thiol or ε-amino group close to or at the ligand binding site of the protein to induce the formation of a covalent bond to site-specifically cross-link the protein and the ligand.[1]

Based on the nature of the reacting amino acid on the protein—whether it is the active site residue of an enzyme or a "non-active site" residue of a nonenzyme protein, we can define two categories of affinity-guided reactions. In the first category, the active site residues of enzyme provide naturally existing reactive groups, so suicide inhibitors, cofactors, or enzyme substrates often serve as the prototype of the reactive ligands. Examples in this category include activity-based protein probes,[2−4] CoA-affinity-based kinase tags,[5] the enzyme-suicide substrate-based SNAP/CLIP-tags,[6,7] the Halo-tag,[8] the lactam-based β-lactamase-tag,[9] and the small molecule inhibitor-based TMP tag.[10,11] In the second category, a "non-active site" residue of a protein that does not possess enzymatic activity serves as the site of bioconjugation; this "non-active site" residue could be a naturally existing residue (e.g., cysteine, lysine, or histidine) or one that has been introduced to a specific site of the protein through structure-guided mutagenesis. One of the most outstanding examples is the development of antibodies with infinite affinity by Meares and co-workers.[12] Monoclonal antibodies which specifically recognize metal-EDTA or metal-DOTA chelates were engineered by mutating selected residues (that are not directly involved in ligand binding but are favorably located close to one end of the ligand) to cysteine. Synthetic antigen derivatives carrying thiol-reactive groups can readily form permanent attachment with the modified antibodies, thereby resulting in infinite affinity.[12−15] Similarly, Hamachi and co-workers utilized a nucleophilic S_N2 reaction between the cysteinyl thiol group of the peptide tags CA6D6 or CA6D4×2 and an α-chloroacetyl attached to Zn(II)-DpaTyr molecules, to achieve spontaneous covalent labeling of proteins.[16,17] Besides cysteines, one can also selectively target lysine residues. For example, Mears and co-workers covalently tethered a 19mer peptide ligand to a unique lysine residue on human vascular endothelial growth factor through a dinitrofluorobenzene group.[18] Kelly and co-workers also showed that ester or thioester derivatives of stilbenes can covalently conjugate with a specific

Received: March 27, 2014
Revised: April 10, 2014
Published: April 16, 2014

lysine residue of transthyretin.[19] Khosla and co-workers also designed peptide analogues containing α-amido aldehyde that can form Schiff base with the ε-amino group of a lysine reside of DQ2 protein.[20] Howarth and others engineered a 13-residue Spytag peptide that can spontaneously and rapidly form a covalent isopeptide bond with the Spycatcher-tagged proteins.[21−23] We recently developed a covalent conjugation reaction based on the specificity of noncovalent coiled coil peptide−peptide interaction and verified the use of the peptide tag for covalent labeling of proteins in solution or receptors on the surface of cells; the reaction was proven to be nonenzymatic, spontaneous, site-specific, and fully biocompatible.[24] These examples manifested that the reversible binding interaction can be converted to covalent bioconjugation reactions through an affinity-guided proximity effect.

These successes notwithstanding, the implementation of affinity-guided reactivity in bioconjugation reactions still lacks thorough exploration. In order to gain the maximum benefit of this principle, we envision that a set of orthogonal bioconjugation reactions can be developed by engineering natural proteins and peptides that possess highly specific interactions. Scaffolding domains in cell signaling are particularly interesting candidates in this regard due to their high specificity for peptide ligands, which is paramount for the regulation of intracellular signals.[25,26] In particular, two types of scaffolding domains, PDZ (PSD-95/Discs-large/ZO-1) and SH3 (Src-homology-3), are natural modular units that constitute multidomain scaffold proteins inside the cell; PDZ and SH3 domains with different combinations can be organized into protein scaffolds onto which other signaling proteins can attach, much like constructing architectures using Lego units.[26] PDZ proteins specifically recognize extreme C-termini of the target proteins,[27−30] and SH3 proteins selectively bind to polyproline peptide sequences.[31−34] Also, both are small in size (PDZ domains have ~100 residues, and SH3 ~60 residues), well-folded, and modular, making them particularly well-suited as tags for protein labeling and assembly. Here we engineered selected PDZ and SH3 domains to establish a set of four new bioconjugation reactions, on the basis of affinity-guided context-dependent reaction between cysteinyl thiol and α-chloroacetyl group of the unnatural amino acid X (Figure 1).[16,17,24] We also thoroughly examined their orthogonality and reported their applications in protein labeling and assembly.

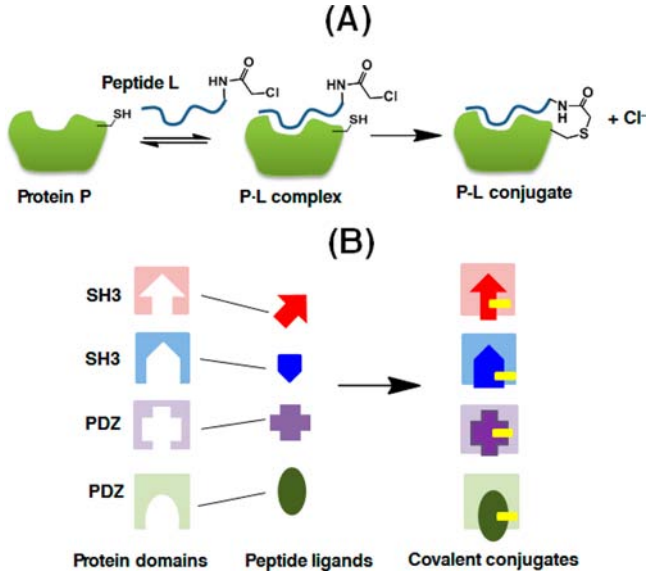

Figure 1. Design of bioconjugation reaction based on affinity-guided reactivity and natural scaffolding domains. (A) The principle of affinity-guided covalent conjugation. The proximity of the two reactive groups in protein P and peptide L induces a nucleophilic reaction to result in a permanent covalent bond, which conjugates the P and L. (B) Engineering four scaffolding domains and their peptide ligands leads to four orthogonal bioconjugation reactions. The yellow patch indicates a covalent linkage between the protein and the peptide ligand.

RESULTS AND DISCUSSION

Structure-Guided Design of Four Bioconjugation Reactions. PDZ1 of the *Drosophila* INAD protein, abbreviated InaD here, specifically binds with a peptide EFCA and forms an intermolecular disulfide bond between Cys31 of InaD and the cysteine of EFCA (Figure 2A).[35−38] We designed a peptide ligand **EFXA**, by substituting cysteine residue of EFCA with the α-chloroacetyl bearing unnatural amino acid **X** (**X** represents (2*S*)-2-amino-3-[(2-chloroacetyl)amino]propanoic acid) and labeling the N terminus with 5(6)-carboxyfluorescein (*fl*) (with an amino acid sequence of *fl*-EFXA). Incubation of **EFXA** with InaD yielded a covalently linked complex that showed as a fluorescent band in the polyacrylamide gel under a fluorescent Typhoon Imager (Figure 2A). The protein complex cannot be dissociated under denaturing condition or in the presence of the reducing reagent DTT, indicating a permanent linkage between InaD and **EFXA**. On the contrary, InaD−EFCA complex disintegrated in the presence of DTT. MALDI-TOF MS analysis also verified the formation of a covalently linked protein−peptide complex with 1-to-1 stoichiometry (Figure S1). Although InaD has two cysteines, Cys31 and Cys62, the conjugation reaction occurred at Cys31 primarily; Cys62 reacted only when **EFXA** is in large excess.

The second bioconjugation reaction was built based on another PDZ protein, Tax-interacting protein-1 (TIP1). Crystal structure of the TIP1−RRESAI complex revealed that Gln43 of TIP1 neighbors the N terminus of the peptide RRESAI with its side chain oriented toward the peptide.[39,40] So, we generated a mutant TIP1^{Q43C} by mutating Gln43 to Cys, and designed the peptide variant ***fl*-XWRE** (having an amino acid sequence of *fl*-XWRESAI), envisioning that in the mutant the thiol group at the side chain of cysteine will adopt similar orientation with the α-chloroacetyl group on the peptide to facilitates an S_N2 reaction (Figure 2B). Expectedly, the purified mutant protein spontaneously formed an irreversible covalent conjugate with the peptide variant after they were incubated together at room temperature or at 37 °C; a fluorescent band corresponding to the molecular weight of the protein complex in Coomassie Blue stained gel image was clearly visible under fluorescent scanner (Figure 2B). In all the reactions, the protein/peptide mixtures were thermally denatured for 10 min at 95 °C before the solutions were loaded on gel to perform SDS-PAGE; therefore, the fluorescent bands shown under fluorescent scanner correspond to covalently bonded complexes between the protein and the peptide, instead of noncovalent reversible binding complexes. To measure the reaction kinetics, we separated aliquots from the reaction solutions at different time points and heated the solutions for 10 min at 95 °C to stop the reactions. The aliquots were then analyzed on denaturing SDS-PAGE to quantify the formation of the protein−peptide covalent complexes at different reaction times. The reaction between InaD and **EFXA** was faster than that between TIP1^{Q43C} and

dx.doi.org/10.1021/bc500134w | *Bioconjugate Chem.* 2014, 25, 989−999

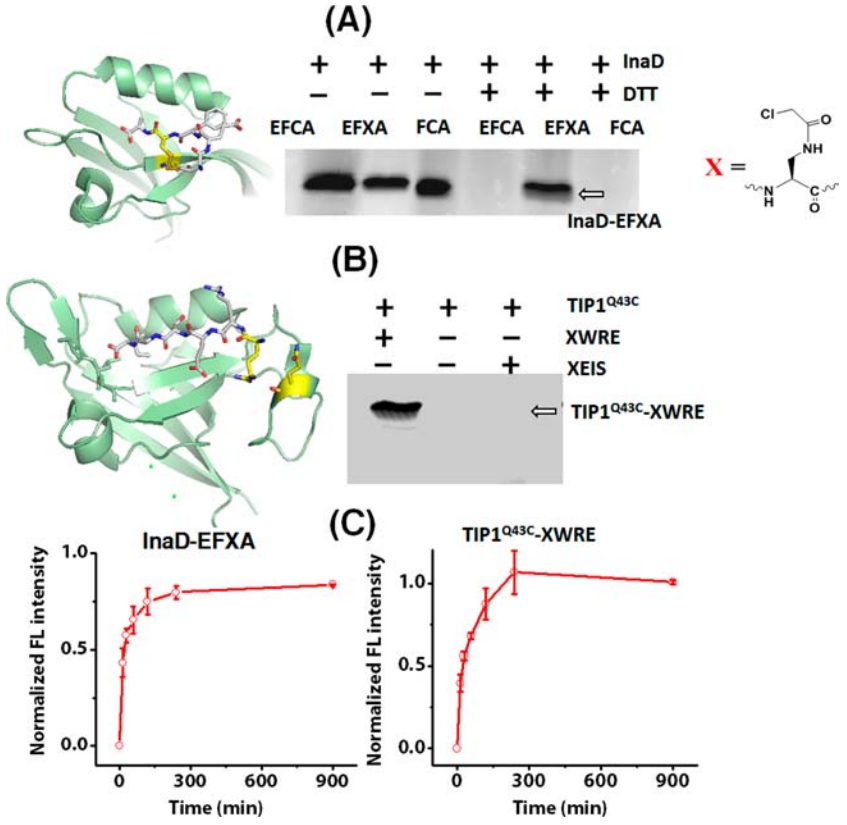

Figure 2. PDZ−peptide covalent conjugations. (A) InaD−**EFXA** conjugation. Crystal structure of the InaD−EFCA complex (PDB entry 1IHJ) shows an intermolecular disulfide bond. The reactions of InaD with fluorescein-tagged **EFCA** (*fl*-EFCA), **EFXA** (*fl*-EFXA), and **FCA** (*fl*-FCA) peptides indicated that a nonreversible bond cross-linked InaD with **EFXA** only. InaD−**EFCA** and InaD−**FCA** complexes dissociated in the presence of DTT. (B) TIP1^{Q43C}−**XWRE** conjugation. Crystal structure of the TIP1−RRESAI complex (PDB entry 3GJ9) suggests Gln43 as mutation site. TIP1^{Q43C} covalently conjugated with *fl*-labeled **XWRE** peptide, but not a control peptide **XEIS** (C) The reaction rate of InaD−**EFXA** and TIP1^{Q43C}−**XWRE** conjugation reactions at 37 °C in PBS ([PDZ] = 10 μM, [peptide] = 40 μM). Fluorescently peptides were incubated with PDZ, denatured, and analyzed by glycine SDS-PAGE with or without DTT. The gels were imaged under a Typhoon scanner (488 nm/520 nm) (Scheme S1). **X** shows the unnatural amino acid (2*S*)-2-amino-3-[(2-chloroacetyl)amino]propanoic acid.

XWRE, with apparent reaction constants k_{obs} measured to be 0.046 min^{-1} and 0.024 min^{-1}, respectively (Figure 2C).

We then applied the same principle to SH3−peptide binding pairs.[31−34] Two SH3 domains that have different binding modes have been chosen as templates. The SH3 domain Abl selectively binds to **p41** peptide, APSYSPPPPP,[41] whereas the SH3 domain Csk binds to **PEP** peptide, PPPLPERTPESFIVVEE.[42] The crystal structure of Abl−**p41** complex shows that Asn31 resides in the vicinity of the N terminus of peptide ligand **p41**, and its side chain points directly toward the peptide. We designed an Abl mutant Abl^{N31C} with Asn31 mutated to Cys, and synthesized the peptide derivative **p41**^{X} (*fl*-**X**PSYSPPPPP) with an X residue installed at the Ala position. Similarly, a Csk mutant Csk^{A40C} and a peptide derivative **PEP**^{X} (*fl*-PPPLPERTPESFI**X**VEE) were designed based on the crystal structure of Csk−**PEP** complex. Upon simple mixing, Abl^{N31C} formed a covalent conjugate with **p41**^{X} (Figure 3A) and Csk^{A40C} covalently cross-linked with **PEP**^{X} (Figure 3B). The reaction rates of these two SH3-based bioconjugation reactions were, however, vastly different. The reaction between Csk^{A40C} and **PEP**^{X} reached 50% completion in about 20 min, but the conjugation between Abl^{N31C} and **p41**^{X} was surprisingly fast: 50% complete in less than 2 min. Fitting the curves into kinetic equations indicated that the Abl^{N31C}−**p41**^{X} conjugation reacted 50 times faster than Csk^{A40C}−**PEP**^{X} (with k_{obs} values measured to be 1.77 min^{-1} and 0.035 min^{-1}, respectively) (Figure 3C). The origin of the rapid covalent conjugation is currently unknown. To provide further evidence that the covalent conjugation reaction was driven by binding affinity, we measured the reaction of Abl^{N31C} with shorter versions of the Abl ligand with progressive truncation at the C terminus after 0.5, 4, and 12 h incubation.[43] Markedly, although all the conjugation reactions reached a similar level of completion after 12 h, at reaction time of 0.5 and 4 h, shorter peptides clearly showed lower yields of conjugated Abl^{N31C}−peptide complex than the longer ones (Figure 4). As longer peptides possess higher binding affinity than the shorter ones, the correlation of binding affinity and conjugation efficiency is consistent with the principle of affinity-guided conjugation.

Orthogonality of the Bioconjugation Reactions. As protein−peptide binding interaction is the prerequisite of covalent reaction, specific protein−peptide interactions should result in orthogonal reacting pairs. Orthogonality means that protein A specifically reacts with ligand A and protein B with ligand B with negligible cross-reactivity. For this purpose, we first examined the cross-reactivity of the two PDZ-based conjugation reactions. Because the two PDZ proteins cannot be clearly resolved on SDS-PAGE, to unambiguously differentiate the two reactions, we utilized two differently labeled peptides, ***fl*-XWRE** labeled with the green dye carboxyfluorescein (*fl*) and ***tmr*-EFXA** peptide (*tmr*-EFXA) labeled with the red dye 5(6)-tetramethylrhodamine (*tmr*). The fluorescent spectra of *fl* and *tmr* are well separated so the conjugate complexes can be

dx.doi.org/10.1021/bc500134w | *Bioconjugate Chem.* 2014, 25, 989−999

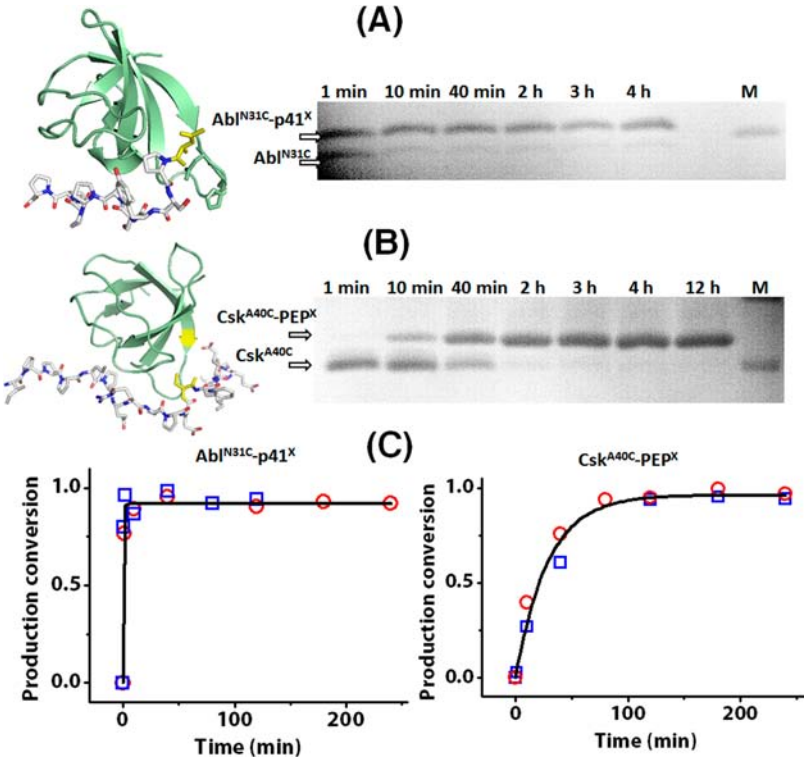

Figure 3. SH3−peptide covalent conjugations. (A) Abl−**p41** conjugation. Crystal structure of the Abl−**p41** complex (PDB entry 1BBZ) shows Gln31 position pointing toward the N terminus of the ligand. Abl^{N31C} reacted with $\mathbf{p41}^{X}$ to form a nonreversible complex. (B) Csk−**PEP** conjugation. Crystal structure of the Csk−**PEP** complex (PDB entry 1JEG) suggests Ala40 as a mutation site. Csk^{A40C} and $\mathbf{PEP}^{X}$ covalently conjugated. (C) The reaction rate of Abl^{N31C}−$\mathbf{p41}^{X}$ and Csk^{A40C}−$\mathbf{PEP}^{X}$ conjugation reactions at 37 °C in PBS ([SH3] = 20 μM, [peptide] = 100 μM). Two independent experiments were shown as blue and red. The data were fitted into kinetic curves. Reaction solutions were denatured, resolved in a tricine-polyacrylamide gel, and stained by Coomassie blue. Lane M shows a marker at 10 kDa.

	Peptide sequence
p40-0	XPTYSPPPPP
p40-1	XPTYSPPPP
p40-2	XPTYSPPP
p40-3	XPTYSPP
p40-4	XPTYSP

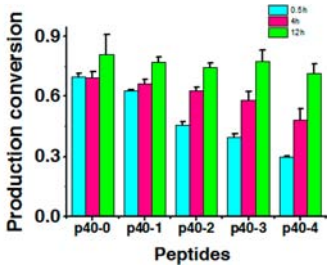

Figure 4. Affinity-dependent reaction rates. Short variants of $\mathbf{p41}^{X}$, listed in the table, showed different reaction rates with Abl^{N31C}. The reactions monitored at 0.5, 4, and 12 h at 37 °C showed that shorter peptides reacted with slower rates but eventually reached a similar degree of completion.

visualized at FITC channel or TRITC channel, respectively. Within the detection limit of the fluorescent scanner Typhoon, we observed that $TIP1^{Q43C}$ reacted only with ***fl*-XWRE**, whereas InaD reacted only with ***tmr*-EFXA** (Figure 5A), showing that the two reactions have minimal cross-reactivity. Similarly, the two SH3-based reactions were also highly orthogonal (Figure 5B). Because the smaller molecular weights of SH3 domains (~60 amino acids), the two bioconjugation reactions on SH3 proteins can be tracked on tricine SDS-PAGE.

After proving the orthogonality within each group, we then examined the overall cross-reactivity of all four reactions. Each of the four fluorescent peptides, **EFXA**, **XWRE**, $\mathbf{p41}^{X}$, and $\mathbf{PEP}^{X}$, was allowed to react with InaD, $TIP1^{Q43C}$, Abl^{N31C}, and Csk^{A40C}, respectively (Figure 5C). Most peptide ligands reacted only with their protein receptors. **EFXA** showed a low level of cross-reactivity with Abl^{N31C} and Csk^{A40C} possibly due to its small size; the reactivity of **EFXA** with Abl^{N31C} and Csk^{A40C} accounted for 12% and 14% of that of **EFXA** with InaD according to the quantification of the fluorescent products (Table 1). Ligand $\mathbf{p41}^{X}$ also showed a low nonspecific reactivity with $TIP1^{Q43C}$. Taken together, the low cross-reactivity is consistent with affinity-guided reactivity, indicating that the specificity of the reversible binding interactions of the wild type protein−peptide pairs has been well preserved in the mutant−ligand pairs, and thereby the binding specificity has been translated into orthogonality of the bioconjugation reactions.

Labeling SH3−Tagged Receptor: Specificity and Biocompatibility. Notably, the conjugation reactions were not affected by the presence of a mixture of proteins in cell lysate. When mixed with cell lysate, ligand $\mathbf{p41}^{X}$ still showed high specificity with Csk^{A40C}, whereas ligand $\mathbf{PEP}^{X}$ selectively reacted with Abl^{N31C}, and no other fluorescent bands were found (lane (1) and lane (7) in Figure 5B). To further illustrate the specificity and biocompatibility, we examined whether these reactions are amenable to a more complex environment under nondenaturing condition during the labeling of cell surface receptor. We tagged a cell-surface receptor with Abl^{N31C} for site-specific labeling. The Abl^{N31C} domain was inserted into the N terminus of the extracellular portion of a modified epidermal growth factor receptor (EGFR) to generate a fusion receptor Abl^{N31C}-*EGFR*.[44,45] When expressed in mammalian cells, the receptor will be transported to the cell membrane, and the extracellular portion, including the Abl^{N31C} tag and HA tag, will be exposed to extracellular space. A *tmr*-labeled p41 peptide, (*tmr*-$\mathbf{p41}^{X}$), as a

dx.doi.org/10.1021/bc500134w | *Bioconjugate Chem.* 2014, 25, 989−999

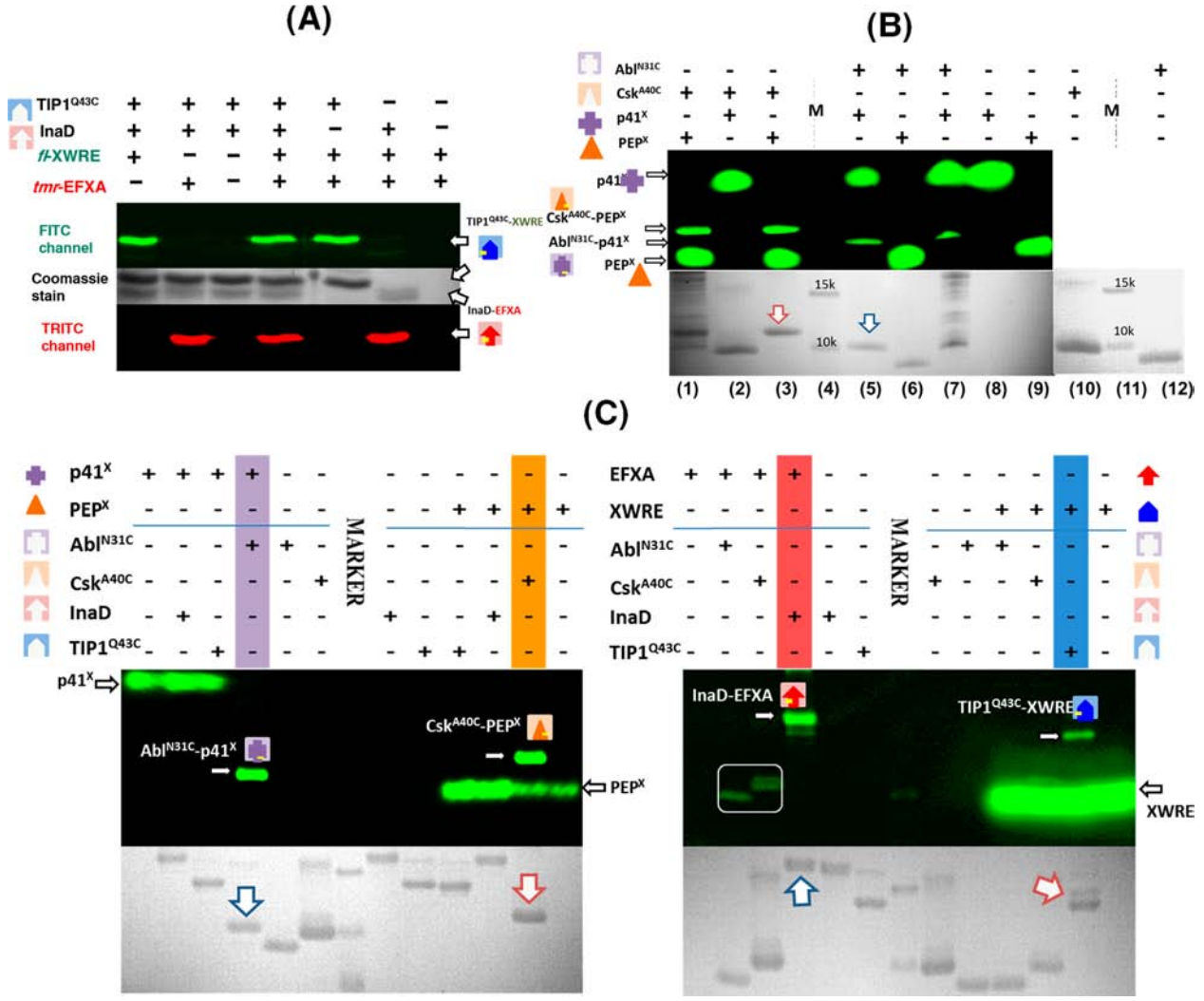

Figure 5. Orthogonality of the bioconjugation reactions. (A) Orthogonality of PDZ−peptide covalent conjugations. *Tmr*-labeled **EFXA** reacted with InaD and *fl*-labeled **XWRE** reacted with TIP1^{Q43C}. The gel was imaged at both FITC and TRITC fluorescent channels before being stained by Coomassie blue. (B) Orthogonality of SH3−peptide covalent conjugations. Peptide **p41^{x}** specifically reacted with Abl^{N31C} and **PEP^{x}** specifically reacted with Csk^{A40C}, shown first by the specific fluorescent bands in fluorescent image (above panel), and second by the increased molecular weights in Coomassie stained image (lower panel). The arrows mark the positions of the complexes. Lanes (4) and (11) are protein markers. Lanes (1) and (7) were reactions in cell lysate. (C) Orthogonality of four domains. The protein gel (tricine SDS-PAGE) was imaged at FITC channel, and stained by Coomassie dye.

Table 1. Quantification of the Cross-Reactivity of Each Protein−Peptide Combination.[a]

	Proteins			
Peptides	Abl^{N31C}	Csk^{A40C}	TIP1^{Q43C}	InaD
p41^{X}	1	0	0.085 ± 0.006	0
PEP^{X}	0	1	0	0
XWRE	0	0	1	0
EFXA	0.123 ± 0.053	0.139 ± 0.022	0	1

[a]The yield of the conjugated complexes after 4 h in each pair, represented by the quantification of the corresponding fluorescent band, was normalized across each row. 0 denotes that cross-reactivity was below the detection limit. Reactions were repeated in triplicates.

probe, can then target the Abl^{N31C} tag specifically, and simultaneously an anti-HA antibody will label the same protein. The pDisplay vector was used to express *Abl^{N31C}-EGFR* in the plasma membrane of Chinese Hamster Ovary (CHO) cells.

CHO cells expressing *Abl^{N31C}-EGFR* were briefly treated with 0.5 mM TCEP for 10 min in cell culture dishes (same as in ref 17) and then were labeled with 2 μM *tmr*-**p41^{X}** in HEPES buffer at pH 7.4 with 0.5 mM TCEP. After the peptide solution was aspirated, the cells were extensively washed with HEPES buffer, fixed by paraformaldehyde, and stained with FITC-labeled anti-HA antibody. Finally, the dishes were extensively washed with PBS buffer and imaged by a confocal microscope. CHO cells expressing *Abl^{N31C}-EGFR* exhibited both green fluorescence (FITC-anti-HA antibody) and red fluorescence (*tmr*-**p41^{X}**) around the plasma membrane, indicating that the Abl^{N31C} tag on EGFR was successfully labeled (Figure 6). Some *tmr* signal was found in the cytosol. It is likely caused by receptor-mediated internalization during peptide labeling on the live cells.[24,44] The fluorescent signal along the transection of a labeled cell also confirmed that the FITC signal and the *tmr* signal colocalized at the plasma membrane (Figure S2). Notably, labeling by the peptide probe persisted after extensive washing steps, indicating

dx.doi.org/10.1021/bc500134w | *Bioconjugate Chem.* 2014, 25, 989−999

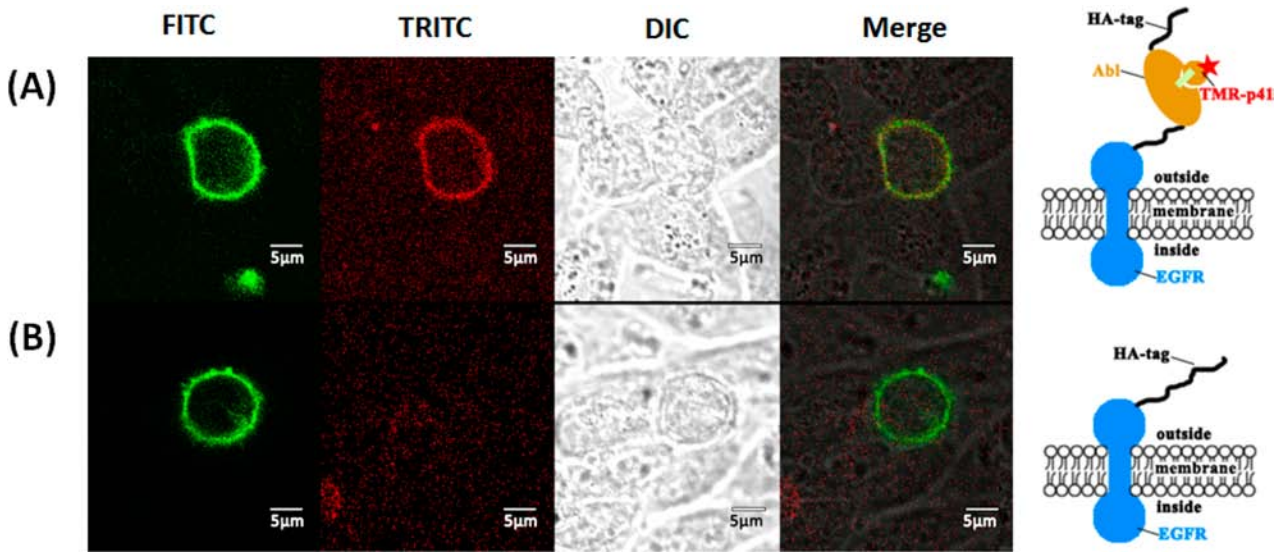

Figure 6. Labeling SH3-fusion protein on cell surface. Confocal fluorescent images of (A) an Abl^{N31C}-EGFR fusion protein and (B) a control EGFR protein without the Abl^{N31C} domain on the surface of CHO cells by peptide probe *tmr*-**p41**^{X}. FITC signal indicates the presence of HA tag; TRITC signal indicates the labeling by *tmr* peptide.

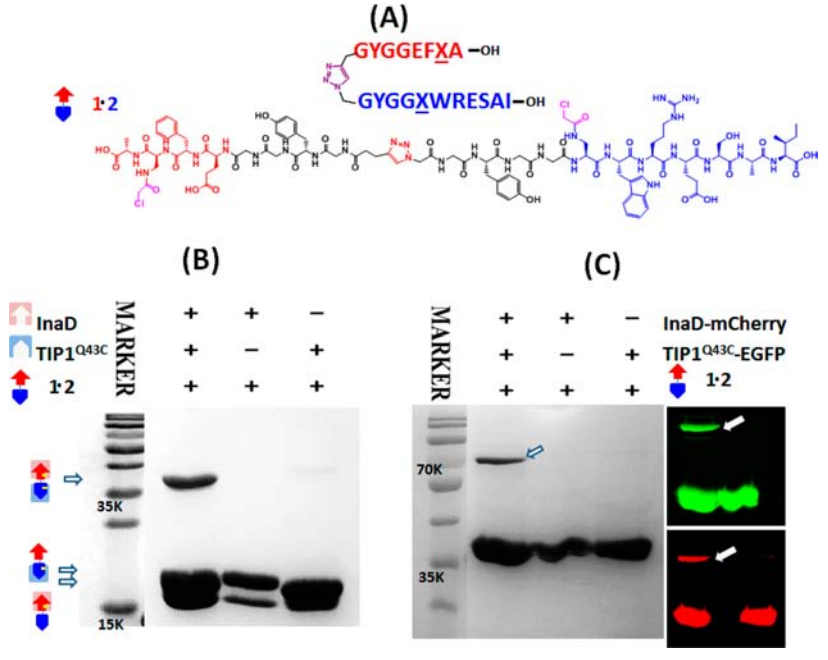

Figure 7. Construction of linear heterodimers using PDZ domains. (A) The structure of **1·2** hybrid peptide. Peptides EFXA and XRESAI were linked through triazole bond at their N termini to form a head-to-head dipeptide **1·2**. (B) InaD and $TIP1^{Q43C}$ formed a heteodimer covalently linked with **1·2** peptide scaffold. (C) Fluorescent fusion proteins InaD-mCherry and $TIP1^{Q43}$-EGFP formed a covalent assembly with **1·2** peptide. The arrows indicate the complex, which showed fluorescent signals at both FITC and TRITC channels in gel.

high specificity and biocompatibility of the bioconjugation reaction.[24]

Construction of Multiprotein Complexes. We then explored the use of the orthogonal protein domains as building blocks to construct multiprotein complexes. A didomain complex with linear geometry was first constructed. We linked peptide fragment **1** (which contains a XWRESAI sequence and an N-terminal azide) with fragment peptide **2** (which contains an EFXA sequence and an N-terminal alkyne moiety) through Cu^{I} catalyzed Click reaction to yield a head-to-head dipeptide **1·2** (Figure 7A) (· denotes a 1,2,3-triazole linkage). When incubated together, InaD and $TIP1^{Q43C}$ reacted with **1·2** spontaneously to give a protein complex shown as a band above 35 kDa in the gel under denaturing condition (Figure 7B), indicating the formation of a heterodimeric complex ($TIP1^{Q43C}$-**1**)·(**2**-InaD) linked through the peptide bridge. To further prove that the complex contains both InaD and $TIP1^{Q43C}$, we reacted **1·2** with fusion proteins InaD-mCherry and $TIP1^{Q43C}$-EGFP which fluoresce at the red or green channel, respectively. A protein complex with a molecular weight matching the sum of the molecular weights of InaD-mCherry, $TIP1^{Q43C}$-EGFP, and the **1·2** peptide was found in the gel under denaturing condition (Figure 7C). The protein complex emits fluorescence at both green and red channels, indicating that both InaD and $TIP1^{Q43C}$

dx.doi.org/10.1021/bc500134w | *Bioconjugate Chem.* 2014, 25, 989−999

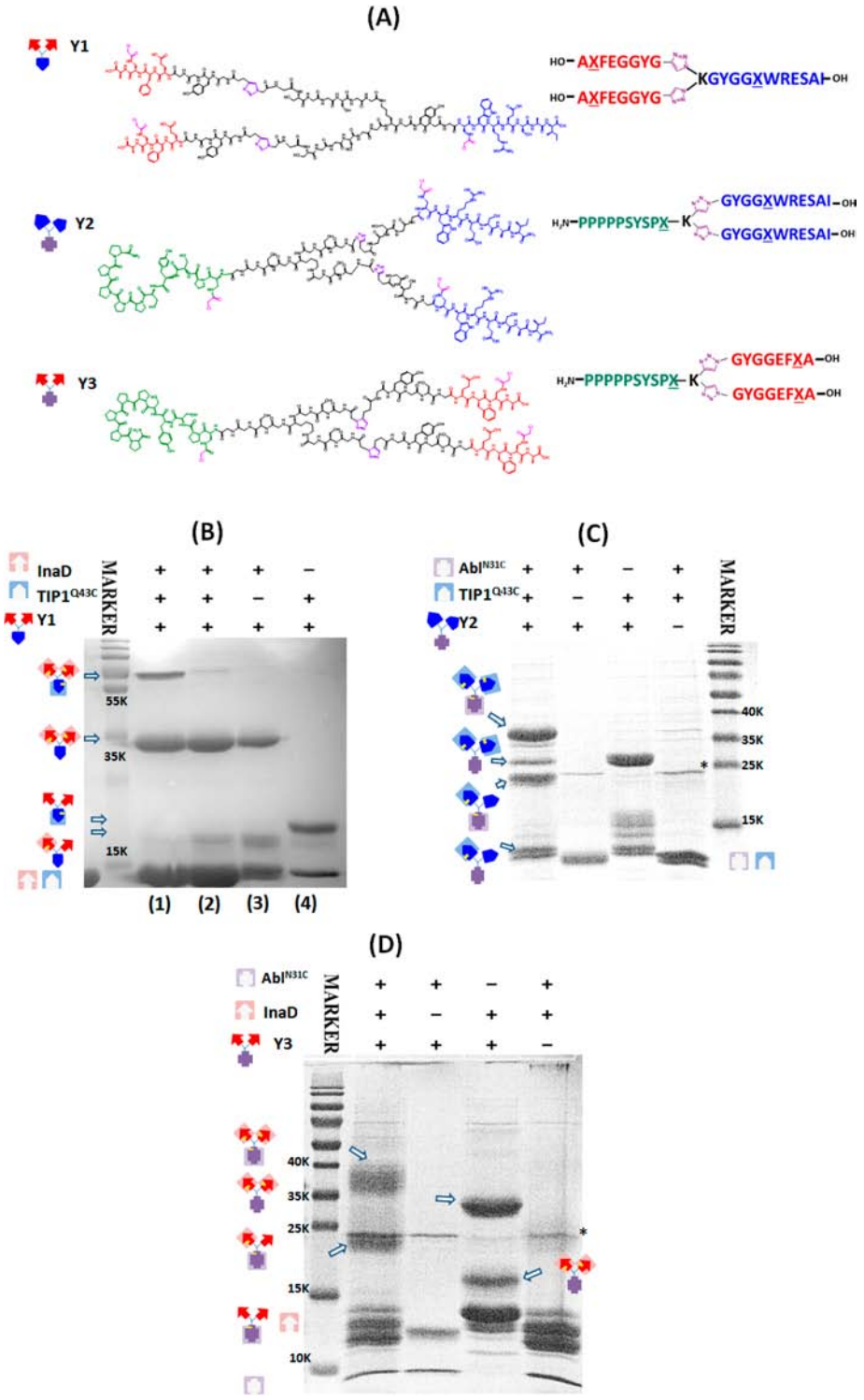

Figure 8. Construction of Y-shaped heterotrimer protein complexes. (A) The structures of Y-shaped peptides **Y1**, **Y2**, and **Y3**. Peptides were linked together by triazole bonds and branched from a lysine site. Note that peptide sequences GYGGEFXA in **Y1** and XPSPSPPPPP in **Y2** and **Y3** are written from C to N terminus in the structures. (B) Two InaD and one TIP1^{Q43C} formed a heterotrimer covalently linked by **Y1**. Lane 2 shows that preincubation of **Y1** with InaD impedes the reaction of TIP1^{Q43C}, suggesting that steric hindrance is a dominant factor. (C) Two Abl^{N31C} and one TIP1^{Q43C} formed a heterotrimer covalently with **Y2**. (C) Two InaD and one Abl^{N31C} formed a heterotrimer covalently with **Y3**. * indicates an impurity.

domains are present in the complex. As the triazole linkage formed by Cu^{I} catalyzed Click reaction is directional, we also synthesized another version of the head-to-head dipeptide **2·1** and obtained essentially the same result (Figure S3).

Last, we constructed heterotrimeric complexes with Y-shaped geometry. A Y-shaped hybrid peptide **Y1**, containing one XWRESAI epitope at the stem and two EFXA epitopes at the forks, was synthesized (Figure 8A). Peptide **Y1** reacted with InaD and TIP1^{Q43C} to yield a covalently linked Y-shaped complex, (InaD-**EFXA**)$_2$·(**XWRE**-TIP1^{Q43C}), above 55 kDa (Figure 8B). Similarly, one Abl^{N31C} and two TIP1^{Q43C} domains formed a covalent heterotrimeric complex on a **Y2** peptide scaffold, which

dx.doi.org/10.1021/bc500134w | *Bioconjugate Chem.* 2014, 25, 989−999

contains two **XWRE** peptides and one **p41**^{X} peptide (Figure 8C). A third case was the assembly of two InaD proteins and one Abl^{N31C} domain assembled on a **Y3** peptide scaffold (Figure 8D). Although some byproducts, mostly dimeric and monomeric complexes, existed in the products, the yield of heterotrimer can be enhanced at higher pH (Figure S4).

CONCLUSION

Bioconjugation reactions that introduce covalent bonds between proteins and ligands on the basis of the principle of affinity-guided reactivity have been widely applied in protein labeling, protein assembly, proteomic studies, covalent inhibitors, and others.[46−51] Despite these successful cases, there still lacks a thorough investigation on the general applicability of affinity-guided reactivity. In other words, the beauty of this concept has not yet been fully exploited, particularly in aspects such as generality and modularity. The first question is whether this strategy is generally applicable: can a protein−peptide interaction be converted into a bioconjugation pair, simply by structure-guided mutagenesis of one residue? The second question is whether binding specificity between the wild-type protein and ligand can be translated to orthogonality of the bioconjugation reactions of the mutant. Here we presented four successful cases which engineered natural protein−peptide interactions of PDZ and SH3 domains and proved the generality of affinity-guided conjugation reactions. Mutation of a residue on the surface of the PDZ or SH3 domain to cysteine allowed a nucleophile to be installed close to the ligand binding site, without harming the folding of the protein. The ligand derivative appended with the electrophilic α-chloroacetyl group binds to the protein mutant in the same way as the wild-type complex, and juxtaposes the two reactive groups in close proximity to induce an S_N2 nucleophilic reaction. The moderate electrophilicity of α-chloroacetyl in aqueous solution is the sine qua non of affinity-guided reaction. Electrophiles with high reactivity, e.g., α-bromoacetyl, will react with all the cysteines in the protein and cysteine-containing small molecules in lysate nonselectively. The α-chloroacetyl group perfectly meets the requirement of affinity-guided reactivity, as only the cysteine in close proximity is involved in the reaction. Besides the α-chloroacetyl group, the acryloyl group as a Michael acceptor of thiol also meets the requirement.[1,11,46] We synthesized acryloyl group containing peptide ligands **EFX′A** and **X′WRESAI**, and found they can also specifically form covalent bonds with the InaD and TIP1^{Q43C}, respectively (Figure S5). Choosing an appropriate site on the protein for cysteine mutation is also crucial for the success of the conjugation reaction. Several factors should be considered. First and foremost, the cysteine should be at a position that is fully exposed to the solvent to ensure its accessibility by the electrophile. Ideally, a loop region has maximal spatial freedom, so the chloride ion, the product of the nucleophilic attack of thiol to α-chloroacetyl, can be readily hydrated and leave the reaction site to allow the reaction to proceed rapidly. Second, the cysteine mutant should preserve most if not all of the original binding affinity of the wild type protein. Therefore, we choose to replace Gln, Asn, or Ala with Cys, respectively, in our cases. Luckily all the cysteine mutations did not seem to drastically affect the protein folding. Adhering to these criteria will then maximize our success of converting a protein−peptide binding interaction into a site specific covalent conjugation reaction. Although two PDZ and SH3 domains were utilized as a proof of principle here, the vast variety of highly specific binding interactions encoded in tightly regulated signaling networks provides almost unlimited choices of templates to engineer orthogonal bioconjugation reactions.[25,26]

We have demonstrated that the bioconjugation reactions can be used for labeling cell surface receptor and constructing multiprotein complexes. Fusion proteins with nonlinear structures and multifunctional attributes are highly desirable, but not technically attainable by genetic engineering of an individual gene. They could be constructed post-translationally through covalent tethering of multiple protein domains that are each individually expressed.[52−57] Post-translational assembly also avoids the risk of misfolding or loss of function of multidomain proteins translated from a single gene. The set of orthogonal and covalent bioconjugation reactions we developed allowed us to construct covalent protein complexes with nonlinear geometry (e.g., Y shape)[54,55,58] in post-translational manner. The protein units can be assembled interchangeably like modules, or Lego units, analogous to the assembly of supramolecular structures using chemical Lego units.[59] It then opens the door to engineering protein devices (such as sophisticated multienzyme complexes) by modular assembly.[60−62] These artificial multienzyme complexes will allow us to probe the enzyme assembly in natural biosynthetic complexes.[56,63] Multifunctional protein complexes can also be used as modulators of cellular functions, or as multimodal imaging probes or delivery vehicle.[52−54] Covalent linkage ensures that the protein units are stably tethered when the protein complex is inside the cell or in serum. Although whether the bioconjugation reactions can be conducted inside cytoplasm still awaits further examination, our strategy greatly expanded the scope of affinity-guided reaction, and provided a system well-suited to dissect its physiochemical mechanism.

MATERIALS AND METHODS

Protein−Peptide Covalent Conjugation Reactions. Purified InaD was incubated with 2-fold excess of *fl*-EFXA, *fl*-EFCA, or *fl*-FCA in PBS at pH 7.4 for 2 h at RT, respectively. The reaction solutions were divided into two identical groups before thermal denaturing. In one group, normal SDS-PAGE loading dye containing DTT was added, whereas in the other group DTT was omitted. Purified TIP1^{Q43C} as mixed with 2-fold of **XRWE** (*fl*-XWRESAI) or a scrambled peptide **XEIS** (*fl*-XEISWRA) as a control, respectively, and incubated in PBS for 2 h at RT. TIP1^{Q43C} in the absence of reacting peptides was also included as another negative control. Purified Abl^{N31C} or Csk^{A40C} was mixed with 5-fold of **p41**^{X} or **PEP**^{X} in PBS and incubated for 2 h at RT. The reaction solutions were then thermally denatured in the presence of loading dye, and resolved by glycine-SDS-PAGE or tricine-SDS-PAGE. The gels were imaged under Typhoon imager at FITC channel. The gels were then stained by Coomassie Blue.

Reaction Orthogonality Examination. The orthogonality of InaD and TIP1^{Q43C} mediated PDZ−peptide bioconjugation reactions was examined using fluorescent peptides **XWRE** (*fl*-XWRESAI) and ***tmr*-EFXA** that carry different fluorescence. Eqimolar InaD and TIP^{Q43C} proteins were mixed with each or both of the two peptides, with a final concentration of 10 μM in PBS, pH 7.4. The reaction solutions were incubated for 2 h at RT before thermal quenching, and resolved by glycine-SDS-PAGE. The gel was then imaged by Typhoon imager at both FITC and TRITC channels and subsequently stained by Coomassie blue.

The specificity of these two SH3 domains was monitored using a similar approach, but with peptides in 5-fold excess. We also included two reaction conditions where the reactions were

performed in a lysate of the *E. coli* homogenate with a protein concentration of 7.5 mg/mL. After being thermally denatured, the solutions were resolved by tricine-SDS-PAGE. The gel was then imaged by Typhoon imager and subsequently stained with Coomassie blue. The specificity of all four domains, InaD, $TIP1^{Q43C}$, Abl^{N31C}, and Csk^{A40C}, were probed using the same approach. Bands corresponding to the respective protein−peptide complexes were identified on the fluorescent image, with the Coomassie staining image as a reference. The fluorescent signal corresponding to each fluorescent band was quantified by ImageJ and the cross-reactivity calculated in Table 1.

Cell Culture, Transfection, and Labeling. Chinese Hamster Ovary (CHO) cells were grown in DMEM/F12 medium (Dulbecco's Modified Eagle Medium: Nutrient Mixture F-12, Life technology, USA) supplied with 10% fetal bovine serum (FBS, Life technology, USA) in a 10 cm culture dish (Corning, USA) and maintained at 37 °C in a humidified incubator supplied with 5% CO_2.

For cell labeling, 1.0×10^5 cells were seeded in a 35 mm confocal dish (ibidi, Germany) 1 day prior to the transfection. At ∼30% confluence, cells were transfected with a DNA (2 μg): FuGENE HD TranfectionReagent (6 μL) mixture at a ratio of 1:3 with the final DNA concentration set to 1 μg/mL in Opti-mem I (Life technology, USA). After 48−50 h, the cells were pretreated with HEPES buffer containing 0.5 mM TCEP for 10 min at RT, and then incubated with fluorescent peptide probes for 30 min. The cells were then washed, fixed by 4% paraformaldehyde in PBS (w/v), and incubated with anti-HA-FITC antibody (in 1:400 dilution) (Sigma-Aldrich, USA) at RT for 1 h. The cells were washed 5 times with PBS (5 min each) and imaged by confocal fluorescent microscope.

Synthesis of Heterodimeric Peptide 1·2, 2·1, and Y-Shaped Peptides Y1, Y2, and Y3. *Peptide 1·2.* Equal equivalents of **1** (azide-GYGGXWRESAI) and **2** (alkyne-GYGGEFXA) were dissolved in H_2O/DMSO (1:1, v/v). 20 equiv of copper sulfate pentahydrate and 40 equiv of sodium ascorbate were added; the solution was stirred overnight in the dark in nitrogen atmosphere. The clicked peptide product **1·2** was purified by semipreparative reverse-phase HPLC, and lyophilized. The identity was confirmed by MS spectra: *m/z* calcd for $[M]^+$ 2283.2, found 2283.7. Peptide **2·1** was synthesized using a similar approach. Equal equivalents of **2** (azide-GYGGEFXA) and **1** (alkyne-GYGGXWRESAI) were dissolved in H_2O/DMSO (1:1, v/v). 20 equiv of copper sulfate pentahydrate and 40 equiv of sodium ascorbate were added; the solution was stirred overnight in dark in nitrogen atmosphere. Peptide **2·1** was found to have the exactly the same molecular mass as peptide **1·2**.

Y-Shaped Peptides Y1, Y2, and Y3. Peptides **5** ((azide-$GSGGSGG)_2$-KGGYGXWRESAI) and **2** (alkyne-GYGGEFXA) in 2-fold excess were dissolved in H_2O/DMSO (1:1, v/v). 40 equiv of copper sulfate pentahydrate and 80 equiv of sodium ascorbate were added; the solution was stirred overnight in the dark in nitrogen atmosphere. The product **Y1** was purified by semipreparative reverse-phase HPLC, and lyophilized. The identity of **Y1** was confirmed by MS spectra: *m/z* calcd for $[M]^+$ 4355.6, found 4356.0. Similarly, Click reaction between peptide **6** ((azide-$GSG)_2$-GSGGXPSYSPPPPP) and **3** (alkyne-GYGGXWRESAI) gave product **Y2**. The identity of **Y2** was confirmed by MS spectra: *m/z* calcd for $[M]^+$ 4726.0, found 4731.7. Click reaction between peptide **6** ((azide-$GSG)_2$-GSGGXPSYSPPPPP) and **4** (alkyne-GYGSGEFXA) gave product **Y3**. The identity of **Y3** was confirmed by MS spectra: *m/z* calcd for $[M]^+$ 4129.6, found 4136.5.

Construction of Multiprotein Complexes. Equimolar mixture of InaD and $TIP1^{Q43C}$ (or InaD-mCherry and $TIP1^{Q43C}$-EGFP) were mixed with 4-fold of heterodimeric peptide **1·2**. Control reactions with each of the reactants (InaD, $TIP1^{Q43C}$, or **1·2**) omitted were also set up in parallel. Final concentration of each PDZ protein was 10 μM, and the final concentration of **1·2** was 40 μM. The reaction solutions were incubated for 3 h at 37 °C before being thermally quenched. Similarly, $TIP1^{Q43C}$ and InaD were mixed with peptide **Y1** with a 1:2:1 ratio, with the final concentration of **Y2** being 20 μM. The reaction solutions were incubated for 6 h at 37 °C in PBS, pH 7.4, before thermal quenching. Also, Abl^{N31C} and $TIP1^{Q43C}$ were mixed with peptide **Y2** at a 1:2:1 ratio, with the final concentration of **Y2** being 20 μM. The reaction solutions were incubated for 6 h at 37 °C in PBS, pH 7.4, before thermal quenching. Further, Abl^{N31C} and InaD were mixed with peptide **Y3** with a 1:2:1 ratio. After incubation, the solutions were quenched by boiling for 10 min, resolved by SDS-PAGE, and stained by Coomassie dye. The conjugation of Abl^{N31C}, $TIP1^{Q43C}$, and **Y2** were also conducted in phosphate buffer buffers with different pH values. Briefly, Abl^{N31C}, $TIP1^{Q43C}$, and Y2 were mixed in 1:2:1 ratio in phosphate buffers with pH values of 7.4, 8, and 9, and incubated at RT overnight. The reaction solutions were resolved in tricine gel (Figure S5).

■ ASSOCIATED CONTENT

Ⓢ Supporting Information

Materials and instruments, the general procedure of peptide synthesis, purification and characterization, information on plasmid construction, protein expression and purification, the general procedure of SDS-PAGE, MALDI-TOF analysis of the complexes. Scheme S1. Figures S1 to S6, and additional characterization data. This material is available free of charge via the Internet at http://pubs.acs.org.

■ AUTHOR INFORMATION

Corresponding Author

*E-mail: jiangxia@cuhk.edu.hk. Phone: (852) 3943 6165. Fax: (852) 2603 5057.

Author Contributions

Yao Lu and Feng Huang contributed equally.

Notes

The authors declare no competing financial interest.

■ ACKNOWLEDGMENTS

This work was partially funded by an Early Career Scheme grant (No. 404812) and a General Research Fund grant (No. 404413) from the Hong Kong Research Grant Council.

■ REFERENCES

(1) Hermanson, G. T. (2008) *Bioconjugate Techniques*, 2nd ed., Academic Press, London.

(2) Cravatt, B. F., and Sorensen, E. J. (2000) Chemical strategies for the global analysis of protein function. *Curr. Opin. Chem. Biol. 4*, 663−668.

(3) Morell, M., Duc, T. N., Willis, A. L., Syed, S., Lee, J., Deu, E., Deng, Y., Xiao, J., Turk, B. E., Jessen, J. R., Weiss, S. J., and Bogyo, M. (2013) Coupling protein engineering with probe design to inhibit and image matrix metalloproteinases with controlled specificity. *J. Am. Chem. Soc. 135*, 9139−9148.

(4) Blair, J. A., Rauh, D., Kung, C., Yun, C.-H., Fan, Q.-W., Rode, H., Zhang, C., Eck, M. J., Weiss, W. A., and Shokat, K. M. (2007) Structure-guided development of affinity probes for tyrosine kinases using chemical genetics. *Nat. Chem. Biol. 3*, 229−238.
(5) Hwang, Y., Thompson, P. R., Wang, L., Jiang, L., Kelleher, N. L., and Cole, P. A. (2007) A selective chemical probe for coenzyme A-requiring enzymes. *Angew. Chem., Int. Ed. 46*, 7621−7624.
(6) O'Hare, H. M., Johnsson, K., and Gautier, A. (2007) Chemical probes shed light on protein function. *Curr. Opin. Struct. Biol. 17*, 488−494.
(7) Gronemeyer, T., Godin, G., and Johnsson, K. (2005) Adding value to fusion proteins through covalent labelling. *Curr. Opin. Biotechnol. 16*, 453−458.
(8) Los, G. V., Encell, L. P., McDougall, M. G., Hartzell, D. D., Karassina, N., Zimprich, C., Wood, M. G., Learish, R., Ohana, R. F., Urh, M., Simpson, D., Mendez, J., Zimmerman, K., Otto, P., Vidugiris, G., Zhu, J., Darzins, A., Klaubert, D. H., Bulleit, R. F., and Wood, K. V. (2008) HaloTag: a novel protein labeling technology for cell imaging and protein analysis. *ACS Chem. Biol. 3*, 373−382.
(9) Mizukami, S., Watanabe, S., Hori, Y., and Kikuchi, K. (2009) Covalent protein labeling based on noncatalytic beta-lactamase and a designed FRET substrate. *J. Am. Chem. Soc. 131*, 5016−5017.
(10) Chen, Z., Jing, C., Gallagher, S. S., Sheetz, M. P., and Cornish, V. W. (2012) Second-generation covalent TMP-tag for live cell imaging. *J. Am. Chem. Soc. 134*, 13692−13699.
(11) Gallagher, S. S., Sable, J. E., Sheetz, M. P., and Cornish, V. W. (2009) An in vivo covalent TMP-tag based on proximity-induced reactivity. *ACS Chem. Biol. 4*, 547−556.
(12) Chmura, A. J., Orton, M. S., and Meares, C. F. (2001) Antibodies with infinite affinity. *Proc. Natl. Acad. Sci. U.S.A. 98*, 8480−8484.
(13) Butlin, N. G., and Meares, C. F. (2006) Antibodies with infinite affinity: origins and applications. *Acc. Chem. Res. 39*, 780−787.
(14) Corneillie, T. M., Whetstone, P. A., Lee, K. C., Wong, J. P., and Meares, C. F. (2004) Converting weak binders into infinite binders. *Bioconjugate Chem. 15*, 1389−1391.
(15) Aweda, T. A., Eskandari, V., Kukis, D. L., Boucher, D. L., Marquez, B. V., Beck, H. E., Mitchell, G. S., Cherry, S. R., and Meares, C. F. (2011) New covalent capture probes for imaging and therapy, based on a combination of binding affinity and disulfide bond formation. *Bioconjugate Chem. 22*, 1479−1483.
(16) Nonaka, H., Tsukiji, S., Ojida, A., and Hamachi, I. (2007) Non-enzymatic covalent protein labeling using a reactive tag. *J. Am. Chem. Soc. 129*, 15777−15779.
(17) Nonaka, H., Fujishima, S., Uchinomiya, S., Ojida, A., and Hamachi, I. (2010) Selective covalent labeling of tag-fused GPCR proteins on live cell surface with a synthetic probe for their functional analysis. *J. Am. Chem. Soc. 132*, 9301−9309.
(18) Marquez, B. V., Beck, H. E., Aweda, T. A., Phinney, B., Holsclaw, C., Jewell, W., Tran, D., Day, J. J., Peiris, M. N., Nwosu, C., Lebrilla, C., and Meares, C. F. (2012) Enhancing peptide ligand binding to vascular endothelial growth factor by covalent bond formation. *Bioconjugate Chem. 23*, 1080−1089.
(19) Choi, S., Connelly, S., Reixach, N., Wilson, I. A., and Kelly, J. W. (2010) Chemoselective small molecules that covalently modify one lysine in a non-enzyme protein in plasma. *Nat. Chem. Biol. 6*, 133−139.
(20) Siegel, M., Xia, J., and Khosla, C. (2007) Structure-based design of a-amido aldehyde containing gluten peptide analogues as modulators of HLA-DQ2 and transglutaminase 2. *Bioorg. Med. Chem. 15*, 6253−6261.
(21) Zakeri, B., Fierer, J. O., Celik, E., Chittock, E. C., Schwarz-Linek, U., Moy, V. T., and Howarth, M. (2012) Peptide tag forming a rapid covalent bond to a protein, through engineering a bacterial adhesin. *Proc. Natl. Acad. Sci. U. S. A. 109*, E690−7.
(22) Zakeri, B., and Howarth, M. (2010) Spontaneous intermolecular amide bond formation between side chains for irreversible peptide targeting. *J. Am. Chem. Soc. 132*, 4526−4527.
(23) Abe, H., Wakabayashi, R., Yonemura, H., Yamada, S., Goto, M., and Kamiya, N. (2013) Split Spy0128 as a potent scaffold for protein cross-linking and immobilization. *Bioconjugate Chem. 24*, 242−250.
(24) Wang, J., Yu, Y., and Xia, J. (2014) Short peptide tag for covalent protein labeling based on coiled coils. *Bioconjugate Chem. 25*, 178−187.
(25) Teyra, J., Sidhu, S. S., and Kim, P. M. (2012) Elucidation of the binding preferences of peptide recognition modules: SH3 and PDZ domains. *FEBS Lett. 586*, 2631−2637.
(26) Nourry, C., Grant, S. G. N., and Borg, J.-P. (2003) PDZ domain proteins: plug and play! *Sci. STKE 179*, re7.
(27) Sheng, M., and Sala, C. (2001) PDZ domains and the organization of supramolecular complexes. *Annu. Rev. Neurosci. 24*, 1−29.
(28) Tonikian, R., Tonikian, R., Zhang, Y., Sazinsky, S. L., Currell, B., Yeh, J. H., Reva, B., Held, H. A., Appleton, B. A., Evangelista, M., Wu, Y., Xin, X., Chan, A. C., Seshagiri, S., Lasky, L. A., Sander, C., Boone, C., Bader, G. D., and Sidhu, S. S. (2008) A specificity map for the PDZ domain family. *PLoS Biol. 6*, e239.
(29) Lee, H.-J., and Zheng, J. J. (2010) PDZ domains and their binding partners: structure, specificity, and modification. *Cell Commun. Signaling 8*, 8.
(30) Huang, A. Y., and Sheng, M. (2002) PDZ domains: structural modules for protein complex assembly. *J. Biol. Chem. 277*, 5699−5702.
(31) Saksela, K., and Permi, P. (2012) SH3 domain ligand binding: What's the consensus and where's the specificity? *FEBS Lett. 586*, 2609−2614.
(32) Kaneko, T., Li, L., and Li, S. S. (2008) The SH3 domain–a family of versatile peptide- and protein-recognition module. *Front. Biosci. 13*, 4938−4952.
(33) Kurochkina, N., and Guha, U. (2013) SH3 domains: modules of protein−protein interactions. *Biophys. Rev. 5*, 29−39.
(34) Li, S. S-C. (2005) Specificity and versatility of SH3 and other proline-recognition domains: structural basis and implications for cellular signal transduction. *Biochem. J. 390*, 641−653.
(35) Kimple, M., Siderovski, D. P., and Sondek, J. (2001) Functional relevance of the disulfide-linked complex of the N-terminal PDZ domain of InaD with NorpA. *EMBO J. 20*, 4414−4422.
(36) Huizen, R. V., Miller, K., Chen, D.-M., Li, Y., Lai, Z.-C., Raab, R. W., Stark, W. S., Shortridge, R. D., and Li, M. (1998) Two distantly positioned PDZ domains mediate multivalent INAD-phospholipase C interactions essential for G protein-coupled signaling. *EMBO J. 17*, 2285−2297.
(37) Kimple, M. E., and Sondek, J. (2002) Affinity tag for protein purification and detection based on the disulfide-linked complex of InaD and NorpA. *BioTechniques 222*, 578−590.
(38) Lichty, J. J., Malecki, J. L., Agnew, H. D., Michelson-Horowitz, D. J., and Tan, S. (2005) Comparison of affinity tags for protein purification. *Protein Expr. Purif. 41*, 98−105.
(39) Zhang, X., Chu, X., Wang, L., Wang, H., Liang, G., Zhang, J., Long, J., and Yang, Z. (2012) Rational design of a tetrameric protein to enhance interactions between self-assembled fibers gives molecular hydrogels. *Angew. Chem., Int. Ed. 51*, 1−6.
(40) Yan, X., Zhou, H., Zhang, J., Shi, C., Xie, X., Wu, Y., Tian, C., Shen, Y., and Long, J. (2009) Molecular mechanism of inward rectifier potassium channel 2.3 regulation by tax-interacting protein-1. *J. Mol. Biol. 392*, 967−976.
(41) Pisabarro, M. T., Serrano, L., and Wilmanns, M. (1998) Crystal structure of the abl-SH3 domain complexed with a designed high-affinity peptide ligand: implications for SH3-ligand interactions. *J. Mol. Biol. 281*, 513−521.
(42) Ghose, R., Shekhtman, A., Goger, M. J., Ji, H., and Cowburn, D. (2001) A novel, specific interaction involving the Csk SH3 domain and its natural ligand. *Nat. Struct. Biol. 8*, 998−1004.
(43) Pisabarro, M. T., and Serrano, L. (1996) Rational design of specific high-affinity peptide ligands for the Abl-SH3 domain. *Biochemistry 35*, 10634−10640.
(44) Nakase, I., Okumura, S., Tanaka, G., Osaki, K., Imanishi, M., and Futaki, S. (2012) Signal transduction using an artificial receptor system that undergoes dimerization upon addition of a bivalent leucine-zipper ligand. *Angew. Chem., Int. Ed. 51*, 7464−7467.
(45) Bill, A., Schmitz, A., Albertoni, B., Song, J. N., Heukamp, L. C., Walrafen, D., Thorwirth, F., Verveer, P. J., Zimmer, S., Meffert, L., Shreiber, A., Chatterjee, S., Thomas, R. K., Ullrich, R. T., Lang, T., and

Famulok, M. (2010) Cytohesins are cytoplasmic ErbB receptor activators. *Cell 143*, 201−211.
(46) Chen, G., Heim, A., Riether, D., Yee, D., Milgrom, Y., Gawinowicz, M. A., and Sames, D. (2003) Reactivity of functional groups on the protein surface: development of epoxide probes for protein labeling. *J. Am. Chem. Soc. 125*, 8130−8133.
(47) Hobert, E. M., and Schepartz, A. (2012) Rewiring kinase specificity with a synthetic adaptor protein. *J. Am. Chem. Soc. 134*, 3976−3978.
(48) Corey, D. R., and Schultz, P. G. (1987) Generation of a hybrid sequence-specific single-stranded deoxyribonuclease. *Science 238*, 1401−1403.
(49) Gartner, Z. J., and Liu, D. R. (2001) The generality of DNA-templated synthesis as a basis for evolving non-natural small molecules. *J. Am. Chem. Soc. 123*, 6961−6963.
(50) Lewis, C. A., and Miller, S. J. (2006) Site-selective derivatization and remodeling of erythromycin A by using simple peptide-based chiral catalysts. *Angew. Chem., Int. Ed. 45*, 5616−5619.
(51) Xiao, J., Broz, P., Puri, A. W., Deu, E., Morell, M., Monack, D. M., and Bogyo, M. (2013) A coupled protein and probe engineering approach for selective inhibition and activity-based probe labeling of the caspases. *J. Am. Chem. Soc. 135*, 9130−9138.
(52) Rossi, E. A., Goldenberg, D. M., and Chang, C.-H. (2012) Complex and defined biostructures with the dock-and-lock method. *Trends Pharmacol. Sci. 33*, 474−481.
(53) Rossi, E. A., Goldenberg, D. M., and Chang, C.-H. (2012) The dock-and-lock method combines recombinant engineering with site-specific covalent conjugation to generate multifunctional structures. *Bioconjugate Chem. 23*, 309−323.
(54) Rossi, E. A., Goldenberg, D. M., Cardillo, T. M., McBride, W. J., Sharkey, R. M., and Chang, C.-H. (2006) Stably tethered multifunctional structures of defined composition made by the dock and lock method for use in cancer targeting. *Proc. Natl. Acad. Sci. U. S. A. 103*, 6841−6846.
(55) Minamihata, K., Goto, M., and Kamiya, N. (2011) Protein heteroconjugation by the peroxidase-catalyzed tyrosine coupling reaction. *Bioconjugate Chem. 22*, 2332−2338.
(56) Schoffelen, S., and van Hest, J. C. M. (2013) Chemical approaches for the construction of multi-enzyme reaction systems. *Curr. Opin. Struct. Biol. 23*, 613−621.
(57) Schoffelen, S., Beekwilder, J., Debets, M. F., Bosch, D., and van Hest, J. C. M. (2013) Construction of a multifunctional enzyme complex via the strain-promoted azide−alkyne Cycloaddition. *Bioconjugate Chem. 24*, 987−996.
(58) Zhang, W. B., Sun, F., Tirrell, D. A., and Arnold, F. H. (2013) Controlling Macromolecular Topology with Genetically Encoded SpyTag-SpyCatcher Chemistry. *J. Am. Chem. Soc. 135*, 13988−13997.
(59) Mathias, J. P., and Stoddart, J. F. (1992) Constructing a molecular LEGO set. *Chem. Soc. Rev. 21*, 215−225.
(60) Whitaker, W. R., Davis, S. A., Arkin, A. P., and Dueber, J. E. (2012) Engineering robust control of two-component system phosphotransfer using modular scaffolds. *Proc. Natl. Acad. Sci. U. S. A. 109*, 18090−18095.
(61) Dueber, J. E., Wu, G. C., Malmirchegini, G. R., Moon, T. S., Petzold, C. J., Ullal, A. V., Prather, K. L., and Keasling, J. D. (2009) Synthetic protein scaffolds provide modular control over metabolic flux. *Nat. Biotechnol. 27*, 753−759.
(62) Anderson, J. C., Dueber, J. E., Leguia, M., Wu, G. C., Goler, J. A., Arkin, A. P., and Keasling, J. D. (2010) BglBricks: A flexible standard for biological part assembly. *J. Biol. Eng. 4*, 1.
(63) Smith, J. L., and Sherman, D. H. (2008) An enzyme assembly line. *Science 321*, 1304−1305.